

# Concentrating Solar Power Systems with Advanced Thermal Energy Storage

Mayank Mani Pandey<sup>1</sup>, Rahul Bahuguna<sup>2</sup>

<sup>1</sup> Faculty of Technology, Uttarakhand Technical University Dehradun, Uttarakhand, India

<sup>2</sup> Assistant. Professor, Dept. of Mechanical Engineering, Faculty of Technology, Uttarakhand Technical University Dehradun, Uttarakhand, India

\*\*\*

**Abstract** - Concentrating Solar Power (CSP) plants have demonstrated the potential to reduce use of fossil fuels to generate electricity. Yet there are limits to the amount of instantaneous renewables penetration due their intermittency. CSP plants coupled with thermal energy storage can reduce solar power intermittency during the day and maintain power output for several hours into the night. This paper describes a CSP plant with storage that uses mixed ionic -electronic conducting metal oxide particles as both the heat transfer and thermal energy storage media. Thermodynamic and economic analyses are reported for a new design of a 4.6 MWe system using solar resource data from Johannesburg, South Africa. A cost comparison is made to local grid power prices to provide a case study for implementing the technology in emerging markets and developing countries. Demonstrated potential reductions in the cost of electricity and peak grid network loading are shown. Results and analyses are contrasted using system-wide metrics, subsystem metrics, and component-level metrics to inform design decisions that increase the societal impact of the sustainable energy system. The leveled cost of electricity produced by the CSP plant is 12 U.S. cents/kW, lower than the average 19 U.S. cents/kWh unsubsidized cost of electricity in sub-Saharan Africa. This work demonstrates the opportunity for a large-scale, renewable, low-cost, and reliable alternative to existing grid power

**Key Words:** solar power, thermodynamics, hydroelectricity

abundant but they do not provide on-demand, dispatchability electric power like hydropower and geothermal generators. Integrating energy storage with solar and wind power improves overall system dispatchability. The inclusion of back-up fossil fuel generation can further increase dispatchability, but this also decreases sustainability. Electricity access is low in sub-Saharan Africa relative to other locations in the world. Currently, only 20% of people in sub-Saharan Africa do not have access to electricity and that number is expected to reach only 40% by 2050. Even areas with an electrified grid are subject to power scarcity issues that decrease wellbeing and limit economic development. For example, industries and manufacturers in sub-Saharan Africa experience an average of 56 days of power outages per year, in comparison to 1 day in 10 years in the United States [2]. The rate of economic growth per capita is expected to increase by an average of 2.2 percent per year if infrastructure and power reliability can be improved [2]. This increase in reliability must also be met with decreases in power prices to further spur development. The average price of electricity in sub-Saharan Africa is an equivalent of 13 U.S. cents/kWh after applying subsidies to reduce the market cost from 19 U.S. cents/kWh [3]. Another issue is the reliance on fossil fuels that exhibit price volatility and contribute to global warming and regional climate change. Large-scale renewable energy sources are an opportunity to address energy issues in sub-Saharan Africa by providing power that is more reliable, more affordable, and more sustainable.

## 2. CONCENTRATING SOLAR POWER

Concentrating Solar Power (CSP) plants can be used to reduce or replace fossil fuel power generation by integrating solar, storage, and gas back-up power into a single generation unit. CSP plants use heat transfer fluids (HTFs) to absorb radiant energy in a solar receiver. This heat can be used immediately to generate power or stored for later use for power generation in off -sun hours. Examples of HTFs include steam, oil, molten salts and phase changing materials (PCM). PCM can store and transfer both

## 1. INTRODUCTION

Emerging economies in Asia, Africa, the Middle East, and Latin America are expected to account for over 90% of the growth in global energy demand [1]. Addressing that growth will require new technologies that provide reliable, affordable, and sustainable sources of energy. Renewables are expected to contribute to an increasingly larger share of global energy supply. Hydroelectric and geothermal resources can provide a steady source of energy for some locations in the world. Solar and wind energy resources are

sensible and latent heat. They also tend to have a higher energy density (gravimetric and volumetric) than sensible heat only materials [4]. PCMs have not replaced synthetic oils or molten salts due to the low power density of commercial-ready PCMs. However, PCMs show promise for Dish-Stirling Engine applications because heat transfer from the material to the engine can be isothermal and occurs simultaneously with the heat transfer of the sun to the material [5,6]. Emerging research in materials that undergo reversible thermochemical reactions can potentially be used as the working fluid and the energy storage media. A redox active metal oxide capable of endothermic reduction followed by exothermic re-oxidation, operates in a two -step cycle: (1) reducing by losing oxygen when the material heats up on sun in a solar receiver and (2) re-oxidizing upon exposure to oxygen (in air). Such a material can be stored hot in reduced form and exposed to air on-demand to produce electricity.

The redox materials in this study are mixed ionic-electronic conducting (MIEC) perovskites ( $ABO_{3-x}$ ). Metal oxides with MIEC properties provide several advantages such as faster reduction and re-oxidation kinetics than non-conducting metal oxides, tunable over a large parameter space (which allows for specific thermodynamic properties to be optimized), and do not undergo major structural rearrangements during re-oxidation or reduction [7]. The stoichiometric balance for reduction and re-oxidation of the perovskite metal oxide is shown in (1) where oxygen is the only additional product and reactant. The reduction extent, symbolized by  $G$ , is a function of the working temperature, partial pressure of oxygen, and the specific material. Further benefits of MIECs are that the redox reactions are not surface limited and the materials are physically stable at elevated temperatures, thereby increasing system efficiency and durability for applications including energy storage [8]. The thermochemical and kinetic properties of MIECs offer transformative potential for energy storage and high efficiency power production in CSP systems. The specific material used in this study is  $CaAl_{0.2}Mn_{0.8}O_{2.9}$  (CAM28). This material has been experimentally measured and characterized by Sandia National Laboratories under the collaborative PROMOTES project [9].

PROMOTES is funded through the DOE SunShot initiative within the ELEMENTS portfolio [10, 11, 12]. Primary goals of the SunShot CSP initiative include increasing system efficiency, reducing power generation cost, and increase system capacity and lifetime. These goals are applicable around the world. Further, CSP design configurations that might be too expensive for the low-cost U.S. energy market could find a

competitive market in emerging economies with higher costs of electricity.

This study introduces an innovative CSP system design of mid-scale size for implementation to urban areas, industrial centers, and peri-urban settlements in sub-Saharan Africa. The proposed CSP design provides low-cost power to reduce consumer electricity expenses, renewable energy to reduce impact on the environment through fossil fuel use, and reliable power to promote economic development in weak grid areas. Thermodynamic and economic analyses are reported for a full CSP system with an air Brayton power cycle.

### 3. TECHNO-ECONOMIC MODEL

The techno-economic model here includes thermodynamic and cost equations. A quasi steady-state thermodynamic equation simulates system operation with hourly time steps for selected days in the year. These intraday results are used to size equipment. Sizing results of the thermodynamic model are then fed into cost calculation equations. Co-optimization for both cost and performance is an ultimate objective pursued planned for future work.

The full system depicted in Fig. 1 includes nine components. The solar field and power block are not included in the closed-loop metal oxide HTF cycle that is comprised of seven components pictured in Fig. 2.

- x The **Solar Receiver Reducing Reactor (SR3)** receives concentrated sunlight from the solar (heliostat) field to heat and drive the endothermic reduction reaction of the metal oxide media.
- x The **Hot Storage (HS) bin** charges with excess reduced particles during sunlight hours and discharges in off-sun hours for on demand power and is connected to a nitrogen pump to isolate stored particles to prevent particle re-oxidation prematurely.
- x Hot reduced particles then pass through the **Re-oxidizer Reactor (ROx)** to exchange oxygen from and heat to a pressurized air stream. The particles and air undergo an exothermic chemical reaction. Particles lose sensible heat and reduce in temperature, and because of the exothermic reaction, the air outlet temperature can be greater than the particle inlet temperature

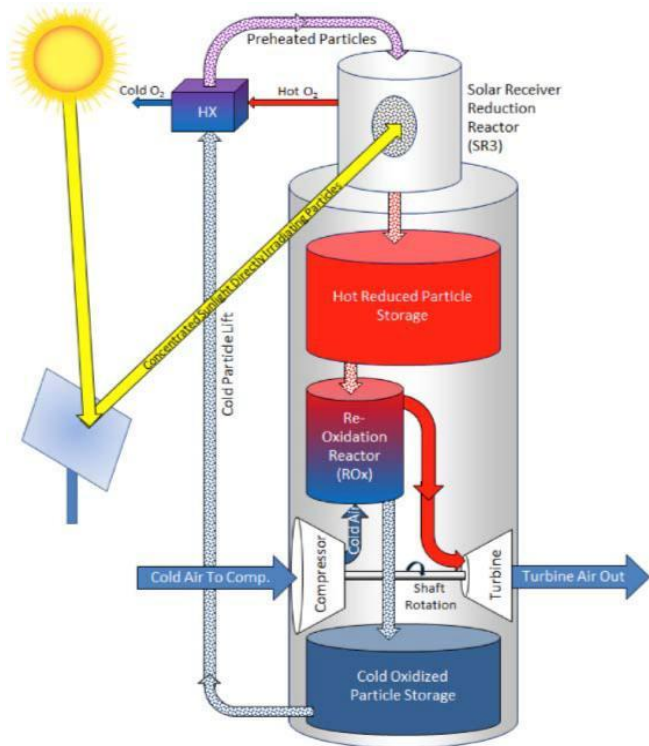


Fig.1. PROMOTES Schematic System Diagram

The extent of reduction  $G$  is a function of the MIEC material, reduction temperature, and partial pressure of oxygen in the SR3. A reduction of  $G=0.206$  is used by fitting the SR3 partial pressure and temperature in thermal gravimetric analysis (TGA). Energy losses from the receiver( 1 ) include re-radiation, convection, and conduction losses. The oxygen flow rate from the SR3 can be calculated using a mass balance from (1), thus ROx heat loss, is based on the surface area of the ROx. The flow of the particles needed to heat up the air in the ROx is back-calculated from the required energy flux entering the ROx, , and flux exiting the ROx, . Those energy state terms are a function of the air flow rate, air temperature, and air pressure, introduced later. If the particles in storage are equal to or surpass the particles needed for electricity production for an hour, particles are discharged from the HS to the ROx

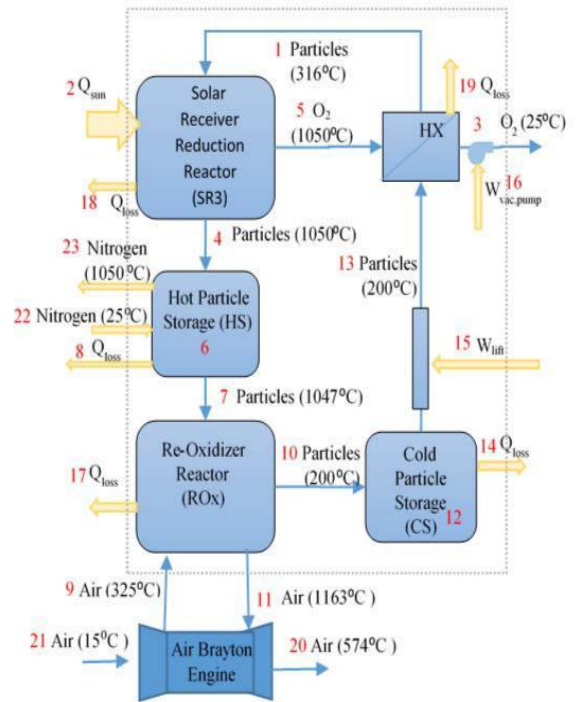


Fig. 2.

The amount of particles in HS is calculated using the previous amount in the bin, charging rate, and discharging rate. Undesired oxidation from air is avoided by pumping nitrogen into the bin to fill unused volume and keep the vessel at ambient pressure. The stored particles and nitrogen are subject to a modest temperature drop during residence time due to conduction and convection losses through the walls. The loss from the bin is calculated from the temperature difference of where again heat capacities are approximated as constants. The HX chosen is a single-pass counter-flow heat exchanger with fluids unmixed. The electrical power for the Vacuum Pump is calculated from the oxygen flow and pressure differential, and assumed efficiency. The electrical power for the particle

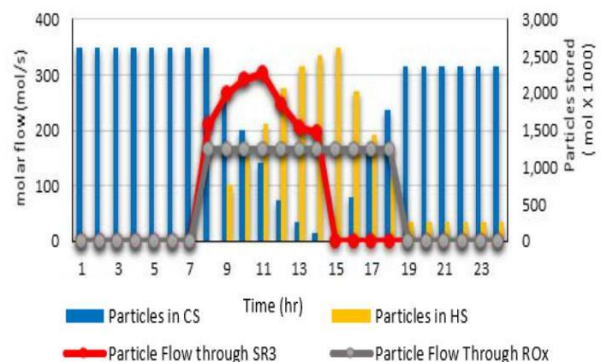


Fig. 3 . Energetic Losses of a 4.6 MWe System at Design Point 900 W/m<sup>2</sup> DNI.

Fig. 4 shows simulated operation with particle flow rate varying over one-day of operation. The particle flow rate through the SR3 varies with changes in DNI. Flow to the SR3 begins when DNI exceeds 350 W/m<sup>2</sup>. The red line beginning at 8 am illustrates the flow of particles through the SR3. This value is directly related to the DNI. At 11 am the DNI reaches the highest DNI of 833 W/m<sup>2</sup>. The grey line indicates the flow of particles through the ROx. Both of the flows begin simultaneously since the energy entering the system surpasses what is needed for power generation. This indicates that electrical generation can begin at 8 am for this system, when the DNI is at 463 W/m<sup>2</sup>. At 3 pm, the DNI fall below 350 W/m<sup>2</sup> and particle flow to the SR3 stops. The yellow bars represent the storage capacity available within HS that allow for a total of 11 hours of power production using only 7 hours of solar.

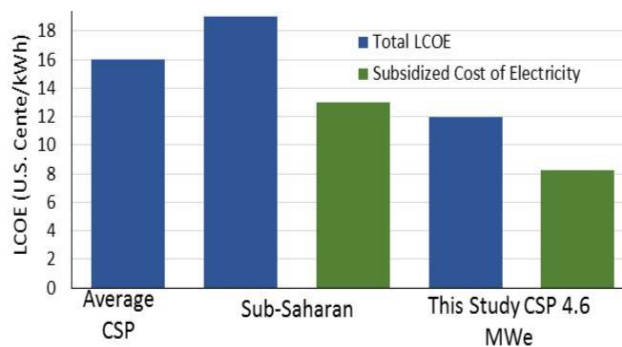


Fig. 4. Intraday particle flow and storage profile for spring solstice (March 20, 1999) in Johannesburg, South Africa with correspondent DNI data shown in W/m<sup>2</sup>.

Fig. 5 illustrates component costs estimated from sizing parameters in Table 2 and associated cost multipliers. Total capital cost of this system is \$22 million. The LCOE estimated for this project is 12 U.S. cents/kWh. The costs were calculated based on a solar field area of 77,096 m<sup>2</sup>, and 2,623,193 moles of particles, which contributes to the majority of the sub-system cost. The estimated cost of solar field, including field preparation, is \$85/m<sup>2</sup>. The cost of raw materials to make particles is \$1 per kilogram for CAM28, multiplied by a fabrication charge that is assumed to be a factor of two.

The replacement of the turbine combustor with the ROx is not taken into account in this design, which means that there can be a decrease in the total component cost. A larger electrical generation capacity may result in the power block fraction of the cost to decrease significantly and its efficiency to increase. Particles remain in HS after the last hour of power generation (hour 19) because there are insufficient particles to operate the power block. The one-hour time step

model could be augmented to run at higher fidelity to include this productivity.

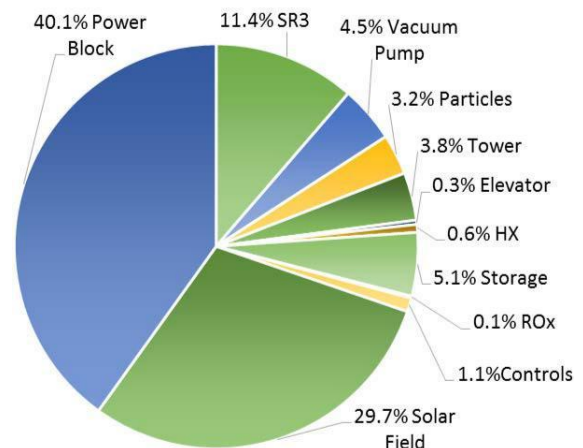


Fig.5. Estimated component contributions for 4.6MWe system using sizing parameters for Johannesburg South Africa.

#### 4. DISCUSSION

This study illustrated an alternative to high-cost, nonrenewable, and unreliable grid power in sub-Saharan Africa by introducing a thermochemical energy storage system coupled to a CSP plant. The solution uses the abundant solar radiation in sub-Saharan Africa to heat metal oxide particles that double as heat transfer fluid in the solar receiver and thermal energy storage media to provide power in on-sun and also off-sun periods.

The estimated LCOE at 12 U.S. cents/kWh is lower than the average cost of electricity in sub-Saharan Africa, with or without subsidies. This illustrates that research and development completed in this study provides evidence for future commercial development and financing of advanced CSP plants that reduce the cost of power. It is useful to note that South Africa's government invested a total of 745 million in energy expenditures in fiscal year 2013/2014 [15]. That amount equates to nearly 34 CSP systems proposed in this study for a combined operating capacity of 156 MWe. Any portion of these funds could be invested in CSP technologies to reduce energy expenditures in the immediate term, reduce future government subsidies, provide additional generation capacity to mitigate black-outs and brown-outs, and increase the use of renewables to reduce fossil fuel exploitation and regional climate change. Such an investment could bring down the cost of delivered energy even further, as illustrated in Fig. 6, if the government

gave the same fractional subsidies as it is awarding for the current generation mix providing grid power.

The majority of system cost comes from the Power Block followed by the Solar Field, as expected. The cost of the Power Block is estimated based on the scaling equations. As previously mentioned, increasing the solar multiple of the system would allow for increased hours of production, however it could also increase the price of the solar field, thus there will be an optimum. In the designed system, a commercial Power Block combustor is replaced by the ROx, in which the particles undergo an exothermic reaction and Fig. 6. Comparison between PROMOTES 4.6 MWe average CSP [16] and sub-Saharan cost of electricity [3].

This cost reduction potential indicates an opportunity to develop and implement advanced CSP systems in developing countries and emerging market economies. Noting, however, certain elements of the technology are yet to be built and demonstrated. The LCOE of the system presented is an average of 4 U.S. cents/kWh lower than most CSP plants and 1 U.S. cent/kWh lower than the average cost of energy in sub-Saharan Africa [3,16]. With subsidies, sub-Saharan African residents pay an average of 13 equivalent U.S. cents/kWh, about 68% of the cost of electricity without subsidies. As illustrated in the green bar in Fig. 6, if the same relative subsidies are given to the CSP plant introduced here, the LCOE cost could reduce to as low as 8 U.S. cents/kWh. This is a compelling case for a renewable and cost-competitive energy source.

## 5. CONCLUSIONS

This case study investigation was completed using solar radiation data for Johannesburg, South Africa. The same system can be used in other locations of sub-Saharan Africa where the solar resource is also strong. Results can be expected to provide similarly low LCOE values in regions with high DNI and long daytime hours. Future work includes modeling different geographical locations and performing sensitivity analysis to select parameters that result in the lowest LCOE and highest energy production.

Such analyses will identify additional markets within sub-Saharan Africa in which this CSP system provides both economic and social benefit.

## REFERENCES

- [1] Weo. "World Energy Outlook." International Energy Agency (2010): 690pp.Web.
- [2] Eberhard, Anton et al. "Underpowered: The State of the Power Sector in Sub-Saharan Africa." *World bank* 6. June (2008): 1-2.Print.
- [3] Alleyne, Trevor. *Energy Subsidy Reform in Sub-Saharan Africa: Experiences and Lessons*. N.p., 2013. Print.
- [4] Glatzmaier, G., 2011. Summary Report for Concentrating Solar Power Thermal Storage Workshop: New Concepts and Materials for Thermal.
- [5] Shabgard, H., Faghri, A., Bergman, T. L., & Andraka, C. E., "Numerical Simulation of Heat Pipe-Assisted Latent Heat Thermal Energy Storage Unit for Dish-Stirling Systems." *Journal of Solar Energy Engineering*, 2014, 136(2), 021025.
- [6] Sharifi, N., Faghri, A., Bergman, T. L., & Andraka, C. E., "Simulation of heat pipe-assisted latent heat thermal energy storage with simultaneous charging and discharging." *International Journal of Heat and Mass Transfer*, 2015, 80, 170-179.
- [7] Miller, J., Ambrosini, A., Coker, E., Allendorf, M., & McDaniel, A., "Advancing Oxide Materials for Thermochemical Production of Solar Fuels." *Energy Procedia* 49 (2014): 2019-26.
- [8] Pardo, P., Deydier, A., Anxionnaz-Minvielle, Z., Rougé, S., Cabassud, M., & Cognet, P., "A review on high temperature thermochemical heat energy storage." *Ren. & Sust. Ener. Rev.*, 2014, 32, 591-610.
- [9] Babiniec, Sean M; Coker, Eric N; Miller, James E; Ambrosini, Andrea; *International Journal of Energy Research*, 02/2016, Volume 40, Issue 2
- [10] U.S. Department of Energy, 2014d. "Project Profile: High Performance Reduction/Oxidation Metal Oxides Thermochemical Energy Storage", from <http://energy.gov/eere/sunshot/project-profile-high-performance-reductionoxidation-metal-oxides-thermochemical-energy>, December 28, 2014.
- [11] U.S. Department of Energy, 2014b. "Concentrating Solar Power", from <http://energy.gov/eere/sunshot/concentrating-solar-power>, December 28, 2014.

- [12] U.S. Department of Energy, 2014c. "Thermal Storage Research and Development for CSP Systems", from <http://energy.gov/eere/sunshot/thermal-storage-rd-csp-systems>, December 28, 2014.
- [13] Robinson, Adam J., comp. Summary of Engine Performance Data - Mercury 50-6400R. N.p.: Solar Turbines Incorporated, 2016. Print
- [14] American Society of Heating, Refrigerating and Air-Conditioning Engineers (ASHRAE), Inc., Atlanta, GA, USA, 2001.
- [15] Pickard, Sam, and Makhijani Shakuntala. "Fossil-fuel Subsidies." World Energy Outlook World Energy Outlook 2014 (2014): 313-44. Web.
- [16] International Renewable Energy Agency (IRENA). "Renewable Power Generation Costs in 2014." Renewable power generation costs (2014): 1- 8. Print.